VIII. MANGANESE NODULE OCCURRENCE AND BENTHONIC ACTIVITIES OBSERVED FROM DEEP SEA PHOTOGRAPHS

Yasumasa Kinoshita, Tomoyuki Moritani, and Keiji Handa

Introduction

Deep sea photographs in the GH77-1 cruise were obtained by two methods, namely a one-shot 16 mm camera attached to the freefall (boomerang) type photo grab and an independent 35 mm deep sea camera. Two freefall photo grabs were routinely used at each station besides a wire-lined larger size grab, Okean-70, to get more accurate data about the population of manganese nodules as well as nodule samples themselves. This freefall photo grab is the product of Preussag Co., West Germany, being attached one shot camera system with an installed 16 mm Minolta camera whose shutter is released by the triggering mechanism due to landing of a suspended weight on the sea bottom. The photographing condition is shown in Table VIII-1. This one shot camera system worked well, and two clear photographs were obtained in each station. These are shown in Fig. VIII-1 (1-14).

Another type of deep sea camera system used consists of Edgerton 35 mm deep sea camera (Model 372) and Deep sea electronic flash (Model 382), both of the products of Benthos Inc., U.S.A. This enabled us to take the continuous photographs of some range of the bottom, at St. 735 (C-11) and St. 737 (C-12). Photographing at St. 735 (C-11) was done at 7 sec intervals for 52 minutes, resulting in 155 frames of clear pictures. From the calculation by magnetic compass simultaneously figured, it is indicated that the ship was drifting towards south with a speed of 0.3 kt, and accordingly that a span of about 500 m length of the bottom was pictured almost continuously. Similarly at St. 737 (C-12), 385 frames of clear pictures of the bottom were obtained by photographing at 7 sec intervals for 63 minutes. In this case, the calculated drifting velocity was 0.2 kt towards

Table VIII-1 Photographing condition.

	35 mm deep sea camera	
Station no.	735(C-11)	737(C-12)
Distance	2 m	2 m
F. stop	5.6	5.6
Film	KODAK PLUS-Pan film black-and-white 100 ft ASA 125	KODAK PLUS-Pan film black-and-white 100 ft ASA 125
Photographing interval	7 sec	7 sec
Photographing time	52 min	63 min
	16 mm camera of freefall photo grab	
Distance	1.2 m	
F. stop	5.6-8	
Film	Minolta 16 black-and-white	

Fig. VIII-1(1-14) Sea bottom photographs by the one shot 16 mm camera of freefall photo grab sampler at each station. The data accompanying each figure indicate station number (St.), observation number (FG = freefall grab), water depth, manganese nodule abundance (in kg/m^2), and scale (10 cm) respectively.

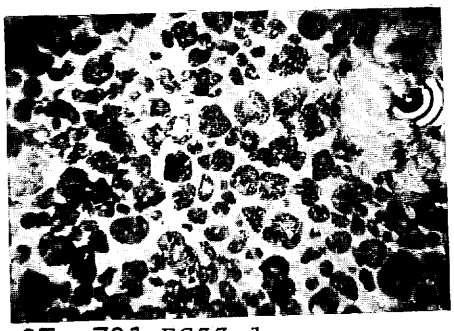

ST. 701 FG33-1
5940m, 3.8kg/m^2 10cm

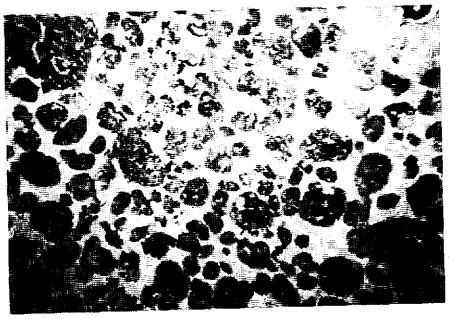

ST. 701 FG33-2
5940m, 17.7kg/m^2 10cm

ST. 702 FG34-1
5900m 10cm

ST. 702 FG34-2
5900m, 12.0kg/m^2 10cm

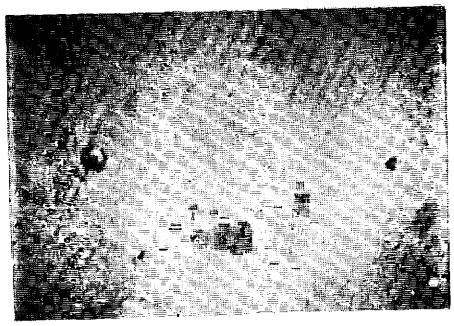

ST. 703 FG35-1
5970m

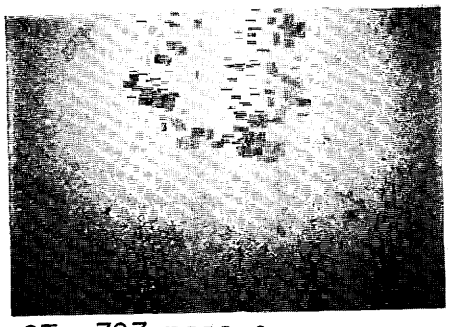

ST. 703 FG35-2
5970m

(1)

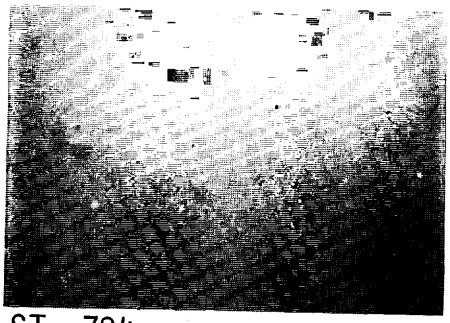

ST. 704 FG36-1
5870m

ST. 704 FG36-2
5870m

ST. 705 FG37-1
5620m, 0.3kg/m^2

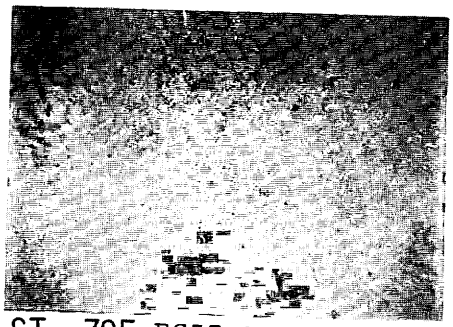

ST. 705 FG37-2
5620m, <0.1kg/m^2

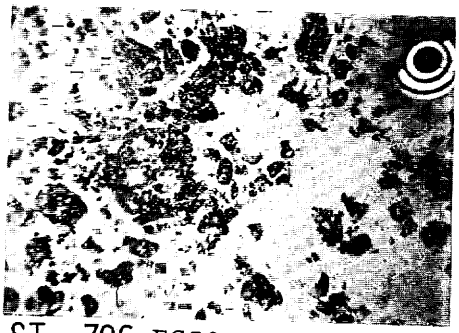

ST. 706 FG38-2
5225m

10cm

(2)

ST. 707 FG39-1
5600m, 10.9kg/m^2 10cm

ST. 707 FG39-2
5600m, 0.2kg/m^2

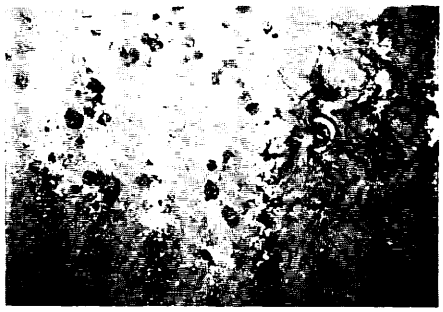

ST. 708 FG40-1
5795m, 2.9kg/m^2 10cm

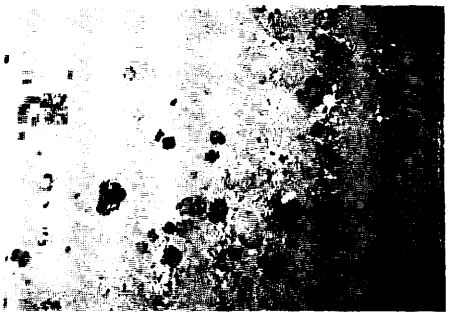

ST. 708 FG40-2
5805m, 2.2kg/m^2

ST. 709 FG41-1
5860m, 0.5kg/m^2 10cm

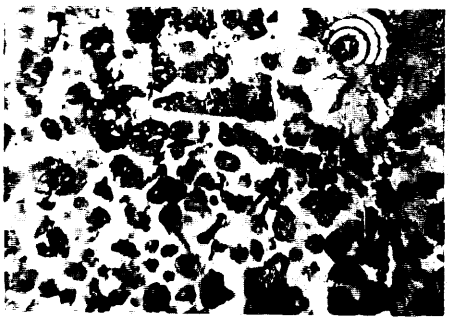

ST. 709 FG41-2
5860m, 2.8kg/m^2 10cm

(3)

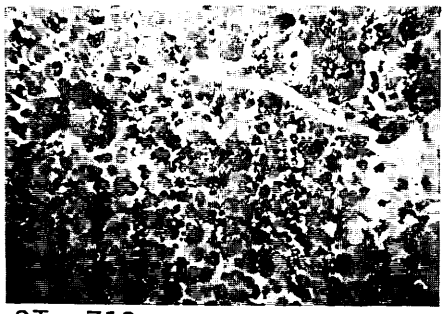

ST. 710 FG42-1
5550m, 11.4kg/m^2 10cm

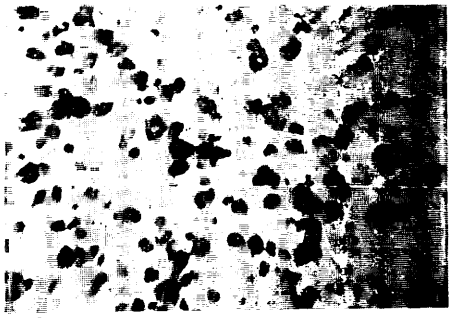

ST. 710 FG42-2
5560m, 2.5kg/m^2

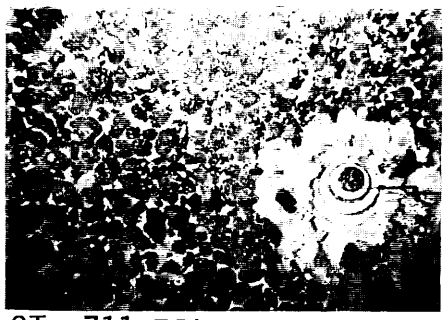

ST. 711 FG43-1
5740m, 15.4kg/m^2 10cm

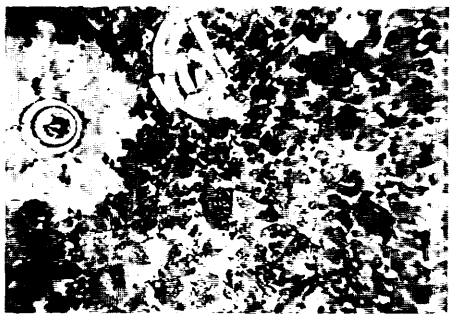

ST. 711 FG43-2
5740m, 0.2kg/m^2 10cm

ST. 712 FG44-1
5900m, 11.3kg/m^2 10cm

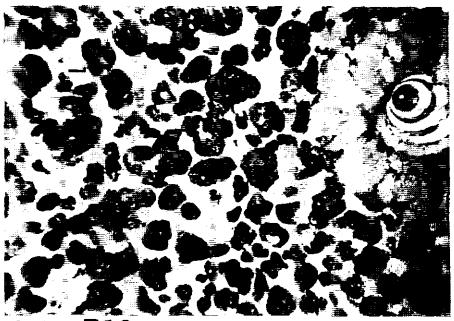

ST. 712 FG44-2
5900m, 1.9kg/m^2 10cm

(4)

ST. 713 FG45-1
5940m, 2.9kg/m^2

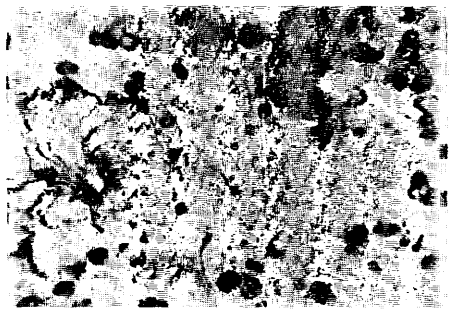

ST. 713 FG45-2
5920m, 0.5kg/m^2 10cm

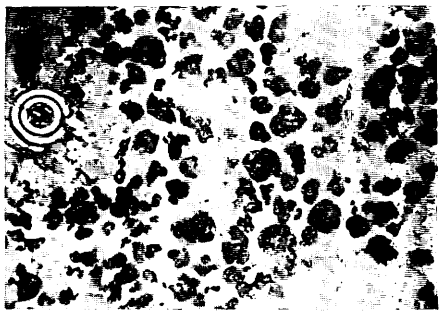

ST. 714 FG46-1
5070m, 9.7kg/m^2 10cm

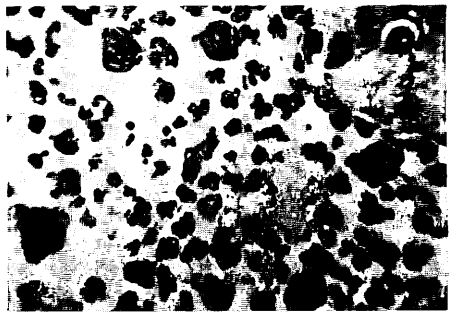

ST. 714 FG46-2
5090m, 1.4kg/m^2 10cm

ST. 717 FG47-1
4018m 10cm

ST. 717 FG47-2
4018m 10cm

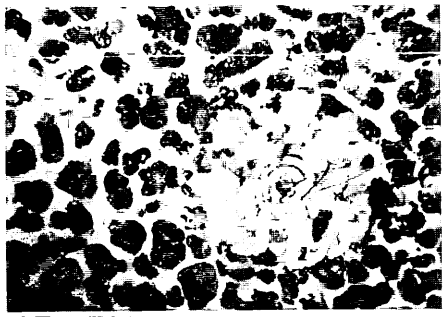

ST. 718 FG48-1
6014m, 17.5kg/m^2 10cm

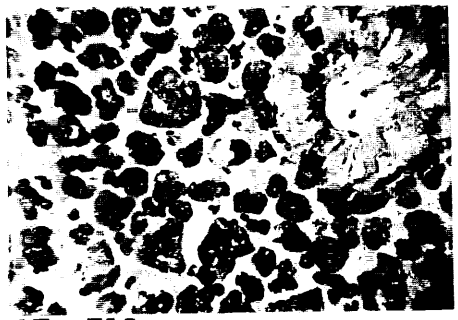

ST. 718 FG48-2
6014m, 20.5kg/m^2 10cm

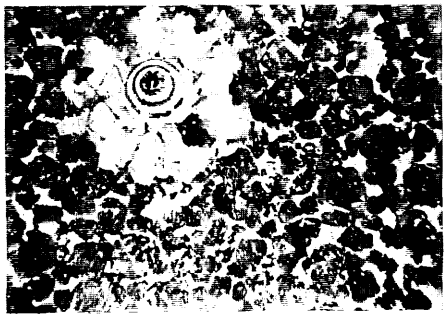

ST. 719 FG49-1
5556m, 26.6kg/m^2 10cm

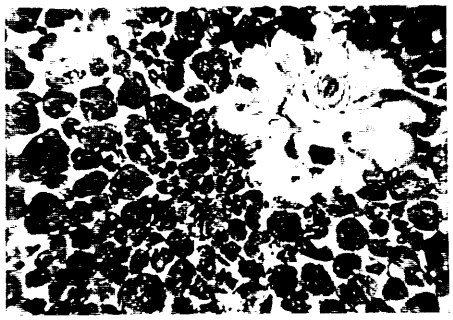

ST. 719 FG49-2
5556m, 16.9kg/m^2 10cm

ST. 720 FG50-1
5346m, 6.5kg/m^2 10cm

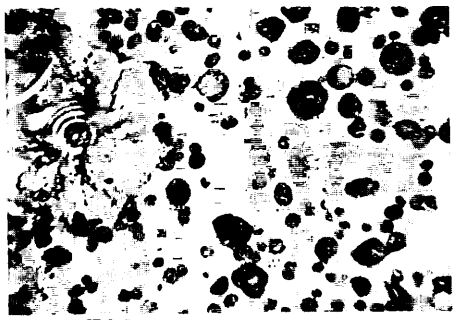

ST. 720 FG50-2
5565m, 4.0kg/m^2 10cm

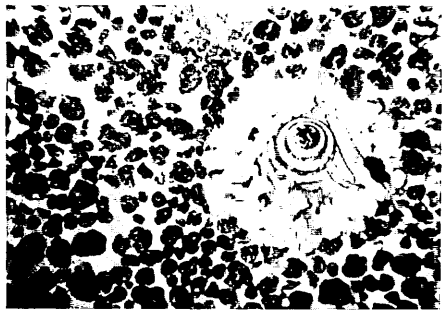

ST. 721 FG51-1
4580m, 7.4kg/m^2 10cm

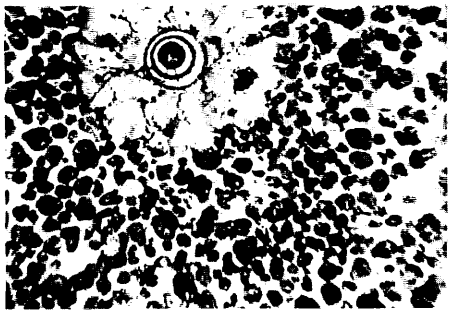

ST. 721 FG51-2
4590m, 4.7kg/m^2 10cm

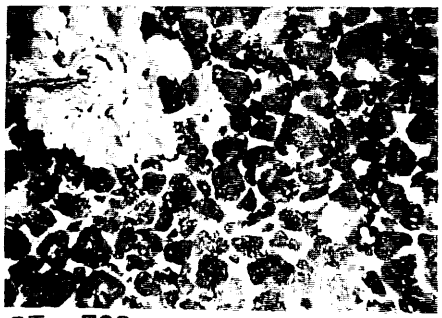

ST. 722 FG52-1
5796m, 28.1kg/m^2 10cm

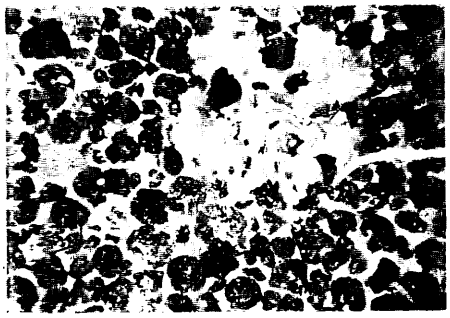

ST. 722 FG52-2
5796m, 23.5kg/m^2 10cm

ST. 723 FG53-1
5952m, 1.4kg/m^2 10cm

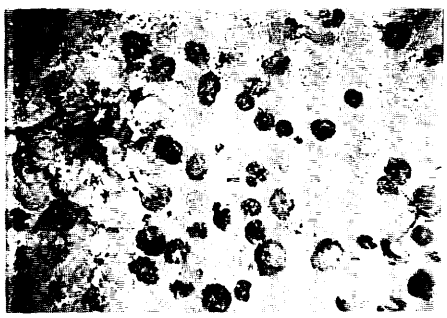

ST. 723 FG53-2
5952m, 2.5kg/m^2 10cm

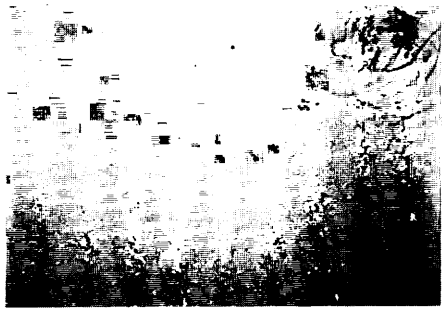

ST. 724 FG54-1
5950m, 0.6kg/m^2

ST. 724 FG54-2
5940m, 0.5kg/m^2

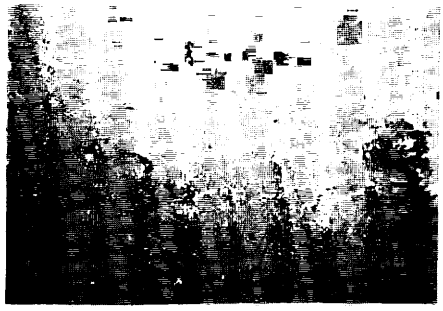

ST. 725 FG55-1
5940m, <0.1kg/m^2

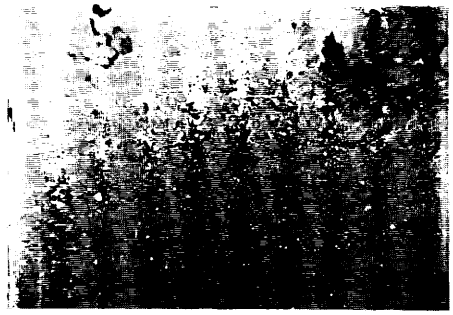

ST. 725 FG55-2
5940m, <0.1kg/m^2

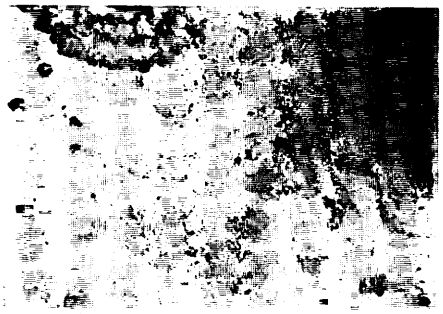

ST. 716 FG56-1
4244m

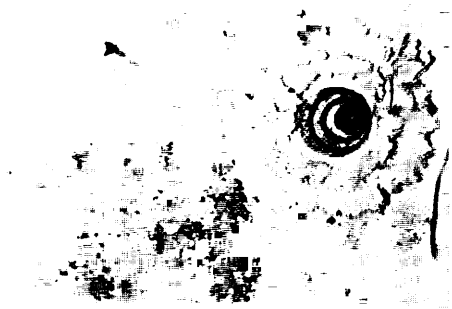

ST. 716 FG56-2
4244m

(8)

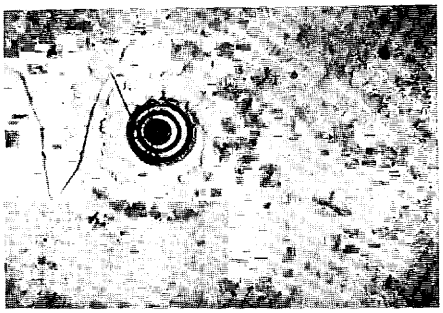

ST. 715 FG57-1
3240m
10cm

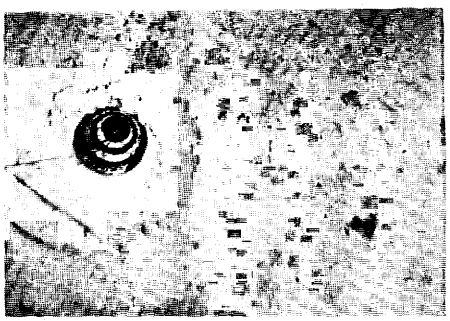

ST. 715 FG57-2
3240m
10cm

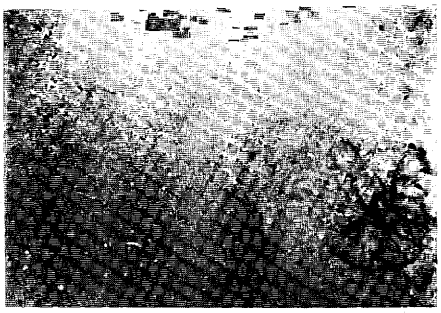

ST. 727 FG58-1
5380m

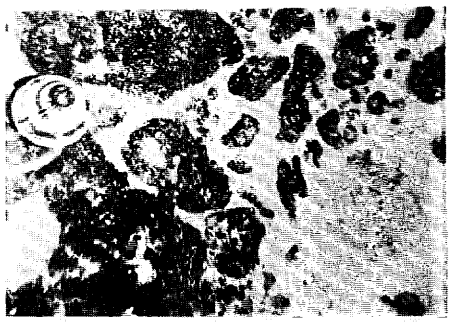

ST. 727 FG58-2
5380m
10cm

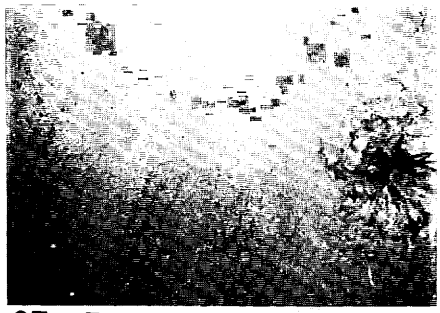

ST. 726 FG59-1
5723m

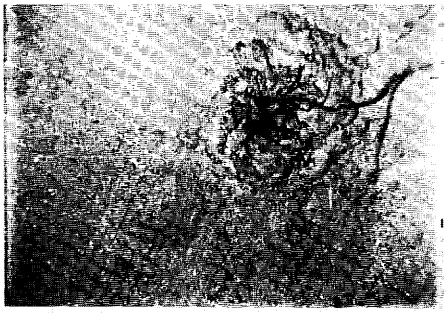

ST. 726 FG59-2
5723m

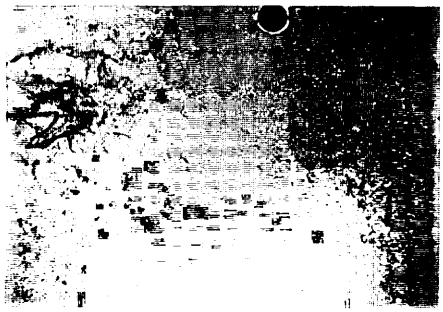

ST. 728 FG60-1
5535m, 0.6kg/m^2

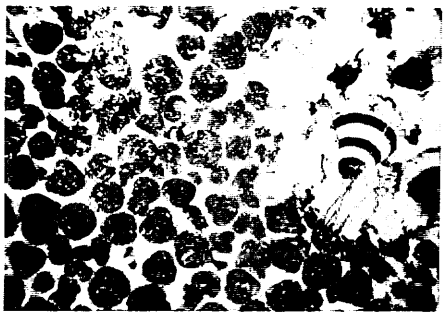

ST. 729 FG61-1
5795m, 25.5kg/m^2 10cm

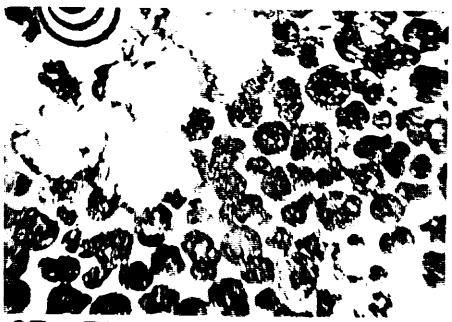

ST. 729 FG61-2
5795m, 19.3kg/m^2 10cm

ST. 730 FG62-1
5865m, 11.5kg/m^2

ST. 730 FG62-2
5865m, 9.7kg/m^2

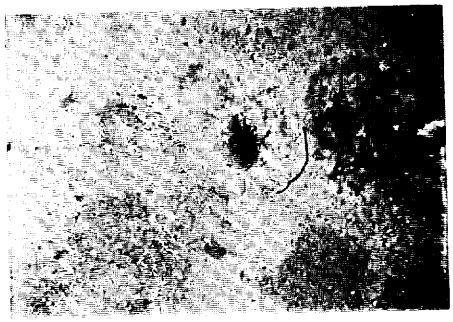

ST. 731 FG63-2
6136m

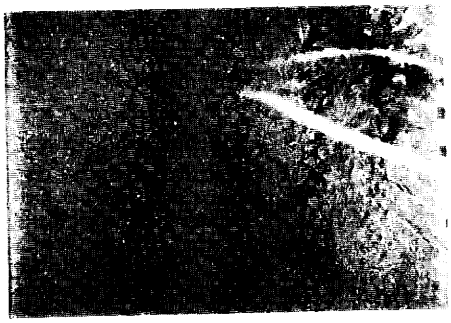

ST. 732 FG64-2
5680m, <0.1kg/m^2

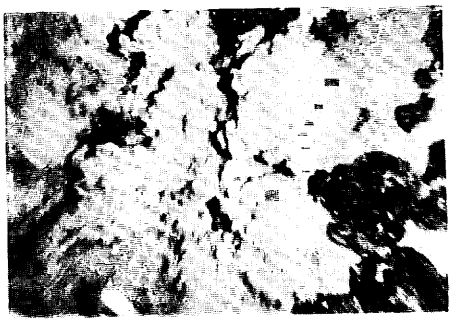

ST. 733 FG65-2
5920m, 24.2kg/m^2

ST. 734 FG66-1
6035m, 10.9kg/m^2

ST. 735 FG67-1
5495m, 27.7kg/m^2 10cm

ST. 735 FG67-2
5484m,<11.9>kg/m^2 10cm

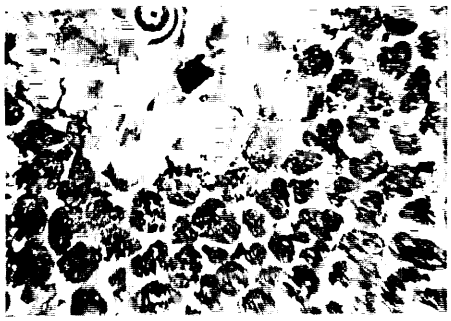

ST. 736 FG68-1
5464m, 27.4kg/m^2 10cm

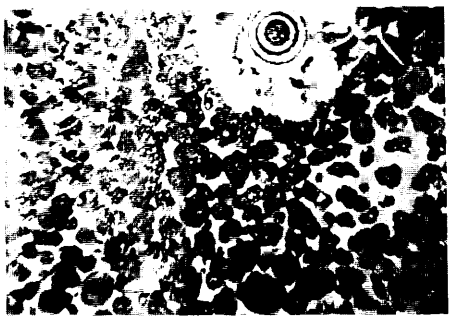

ST. 736 FG68-2
5464m, 26.5kg/m^2 10cm

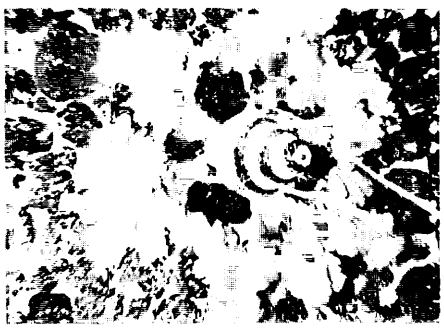

ST. 737 FG69-1
5743m, 23.6kg/m^2 10cm

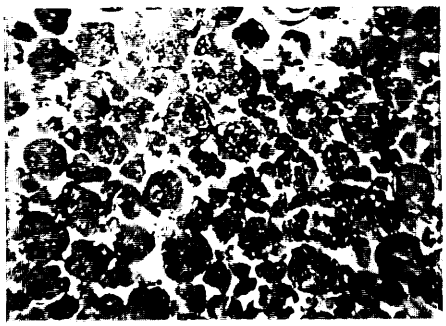

ST. 737 FG69-2
5743m, 26.1kg/m^2 10cm

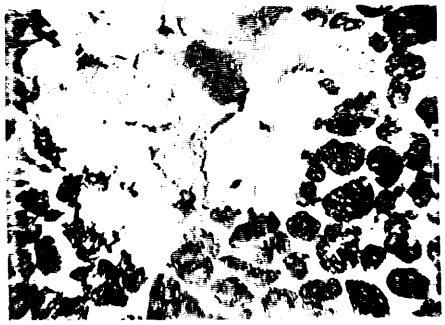

ST. 738 FG70-1
6140m, 14.6kg/m^2 10cm

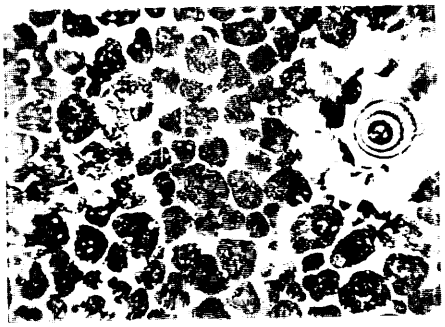

ST. 738 FG70-2
6150m, 26.2kg/m^2 10cm

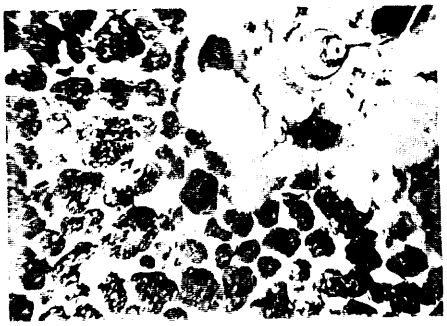

ST. 719A FG71-2
5785m, 23.5kg/m^2 10cm

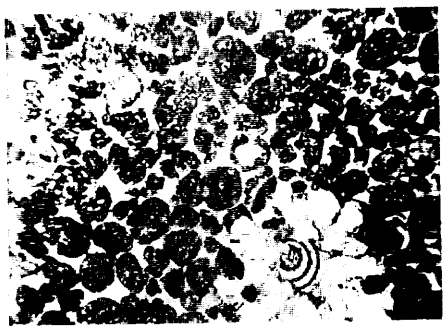

ST. 719A FG71-4
5815m, 23.6kg/m^2 10cm

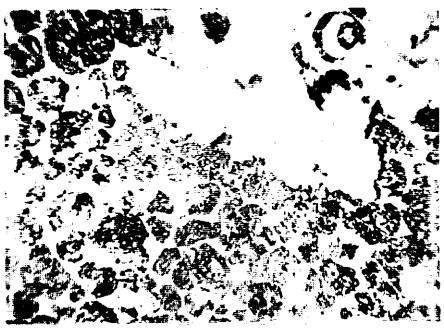

ST. 719A FG71-7
5484m, 26.1kg/m^2 10cm

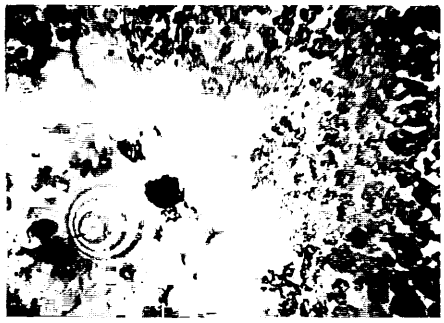

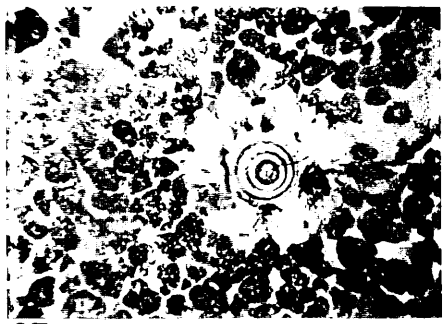

south–southwest, and then the pictured range of the bottom area was estimated as about 355 m.

Each one picture from St. 735 and St. 737 is shown in Fig. VIII–2 and Fig. VIII–3 respectively. On obtained photographs, cover ratio and grain size distribution of manganese nodules, and evidences of benthonic activity were observed. Some results are discussed below.

Cover ratio

The cover ratio of manganese nodules on the photographs both from the freefall photo grab and 35 mm deep sea camera was determined by means of comparison with color index chart. The results are shown in Fig. VIII–4. Higher ratio is found in the northern zonal area between 9°–11°N latitudes, trending in WNW–ESE.

Especially, the values at Sts. 737, 739, 719,736, 722, and 735 show the highest level of 70–75%. Two respective photographs at each station generally showed the same or similar ratio. But, in some cases, the abrupt changes in cover ratio were observed even within the same station area, namely within the short distance of a few hundred meters. For examples, there were recognized differences in ratio as 65% and 8% at St. 710 of the northernmost area, and 30% and 2% at St. 707. On the other hand, scarce or no nodules were found often in the relatively flat basin area and at the top of Magellan Rise.

Grain size distribution of manganese nodules

The size of manganese nodules was measured on the photographs obtained at each station for the grain sizes of 8–6 cm, 6–4 cm, 4–2 cm and less than 2 cm, and then the percent of each size class was calculated. The results are shown in Fig. VIII–5—8.

8–6 cm grain size nodules show the highest values of 15.3% at St. 718 and 8.5% at St. 718, while at other stations it is less than 5%. 6–4 cm grain size nodules show the highest values of 20–30% along the higher cover ratio area, but the percentage decreases towards the northernmost part and the central part to the south respectively. 2–4 cm grain size nodules are most abundant in all stations except St. 737, showing the level of 50–60%. Nodules smaller than 2 cm grain size are less than 20% along the area of the higher cover ratio, but the percentage increases towards the marginal parts of the area.

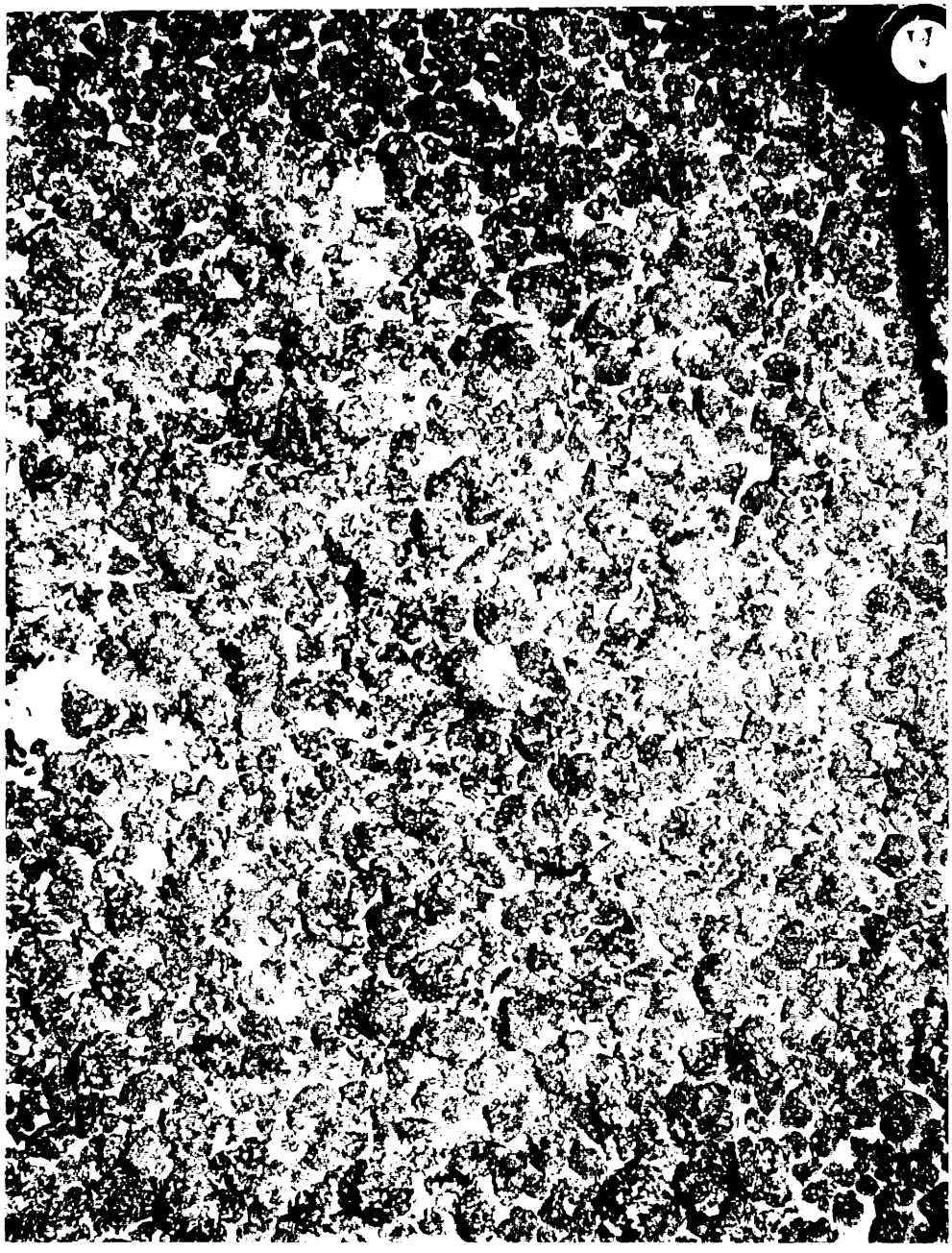

Fig. VIII–2 Sea bottom photograph by 35 mm deep sea camera at St. 735. The data show observation no. (C–), water depth and manganese nodule abundance (kg/m²) by freefall grab sampling.

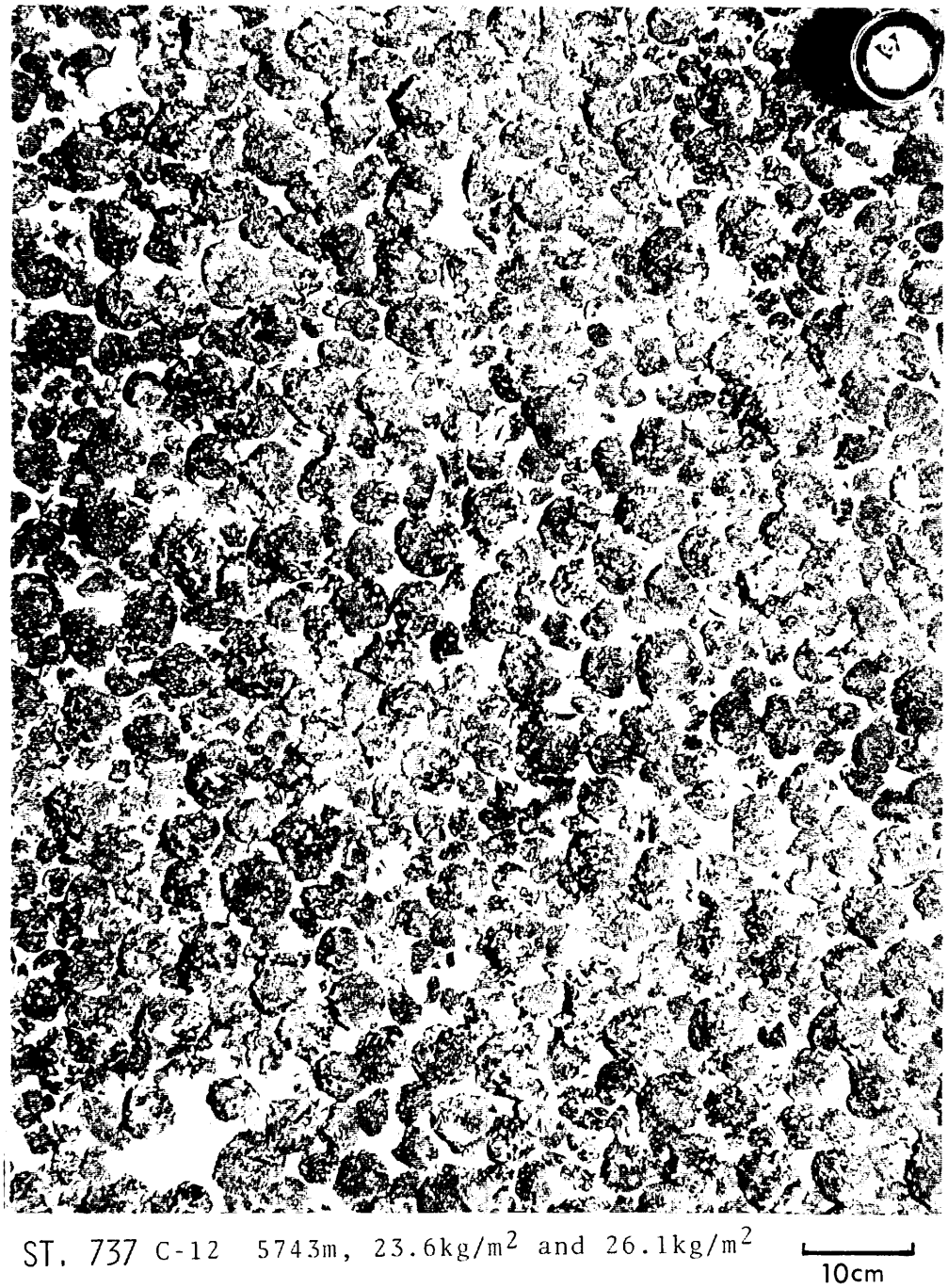

Fig. VIII–3 Sea bottom photograph by 35 mm deep sea camera at St. 737.

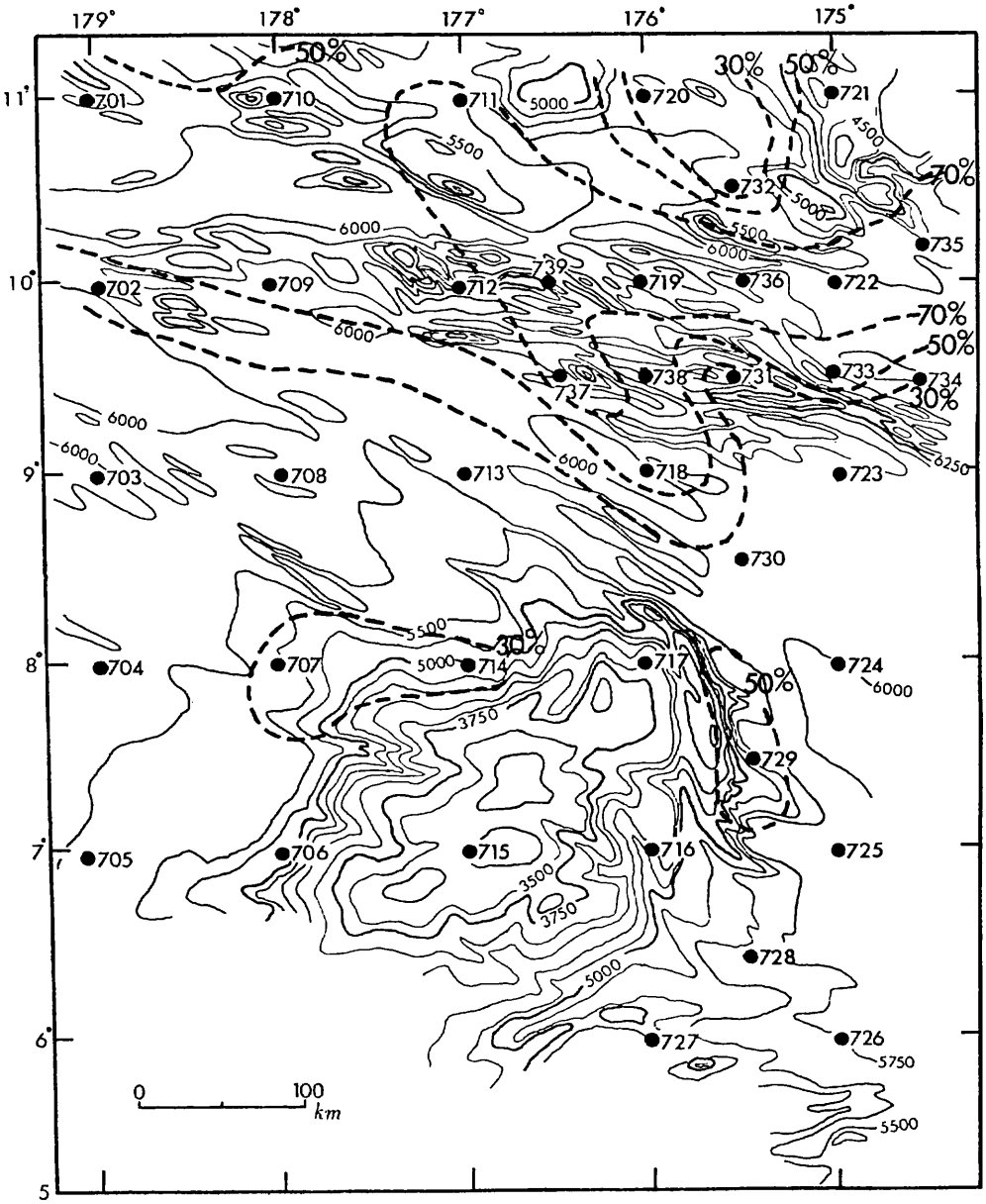

Fig. VIII–4 Cover ratio of manganese nodules.

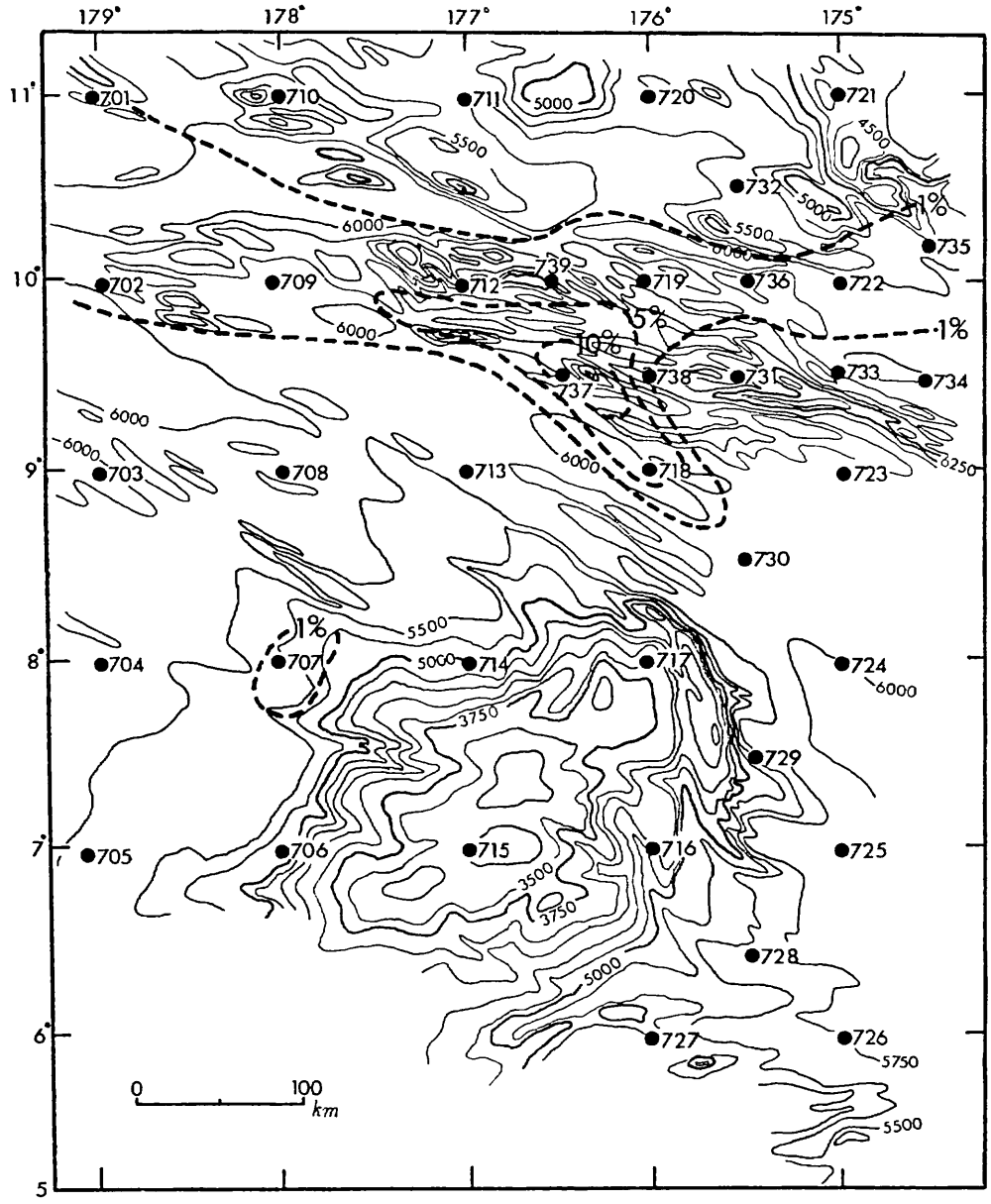

Fig. VIII–5 Grain size distribution of 8–6 cm manganese nodules.

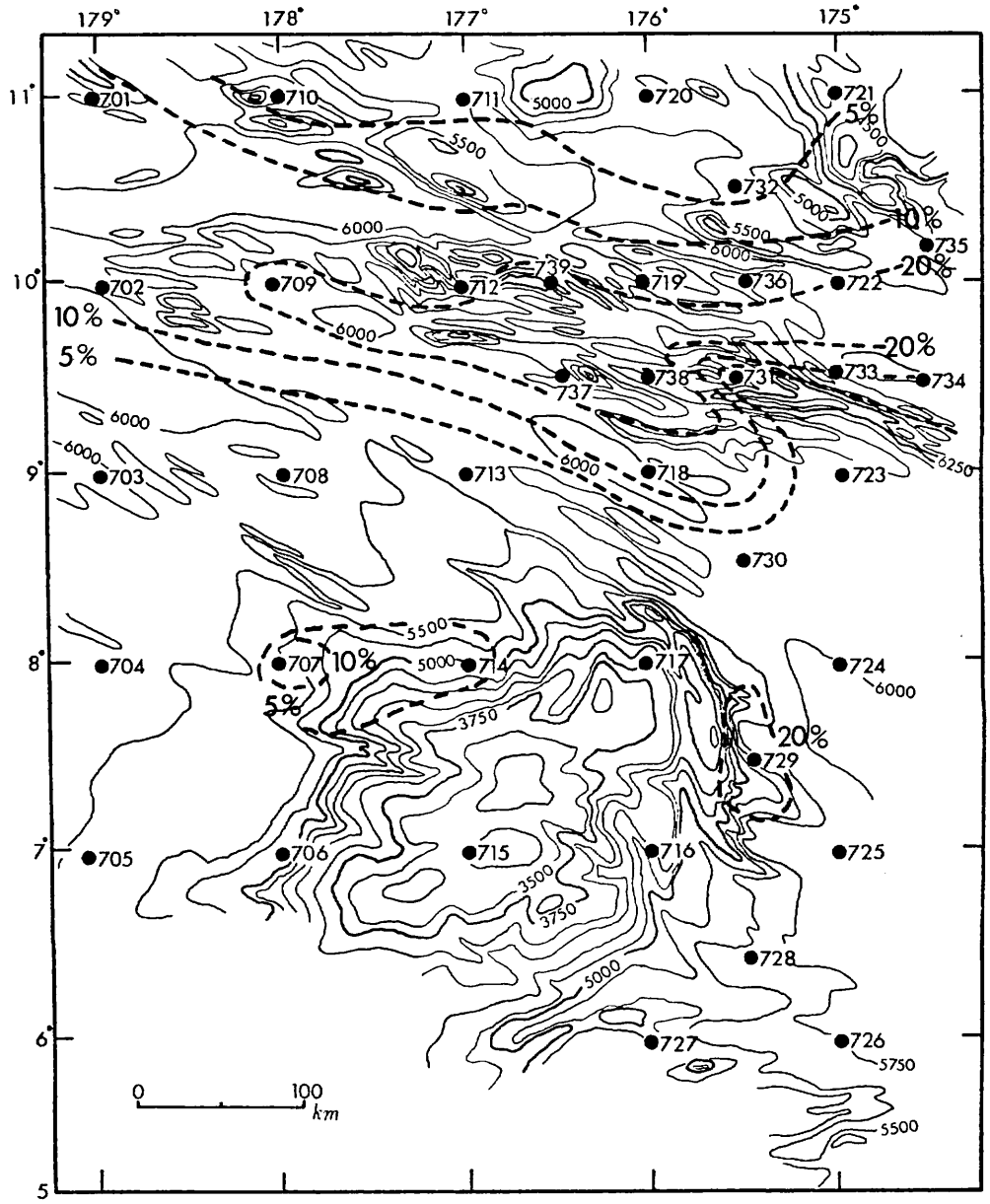

Fig. VIII–6 Grain size distribution of 6–4 cm manganese nodules.

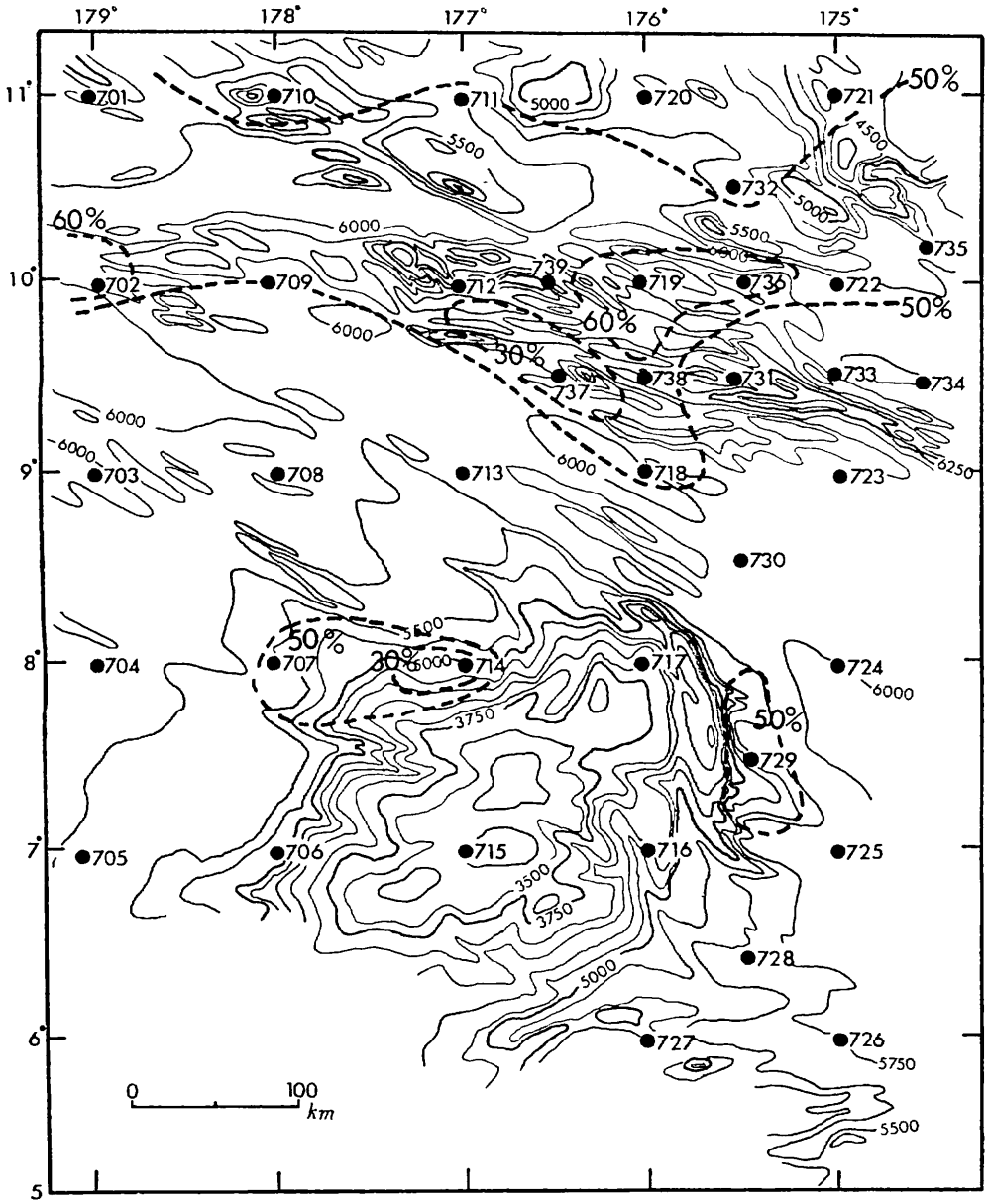

Fig. VIII–7 Grain size distribution of 4–2 cm manganese nodules.

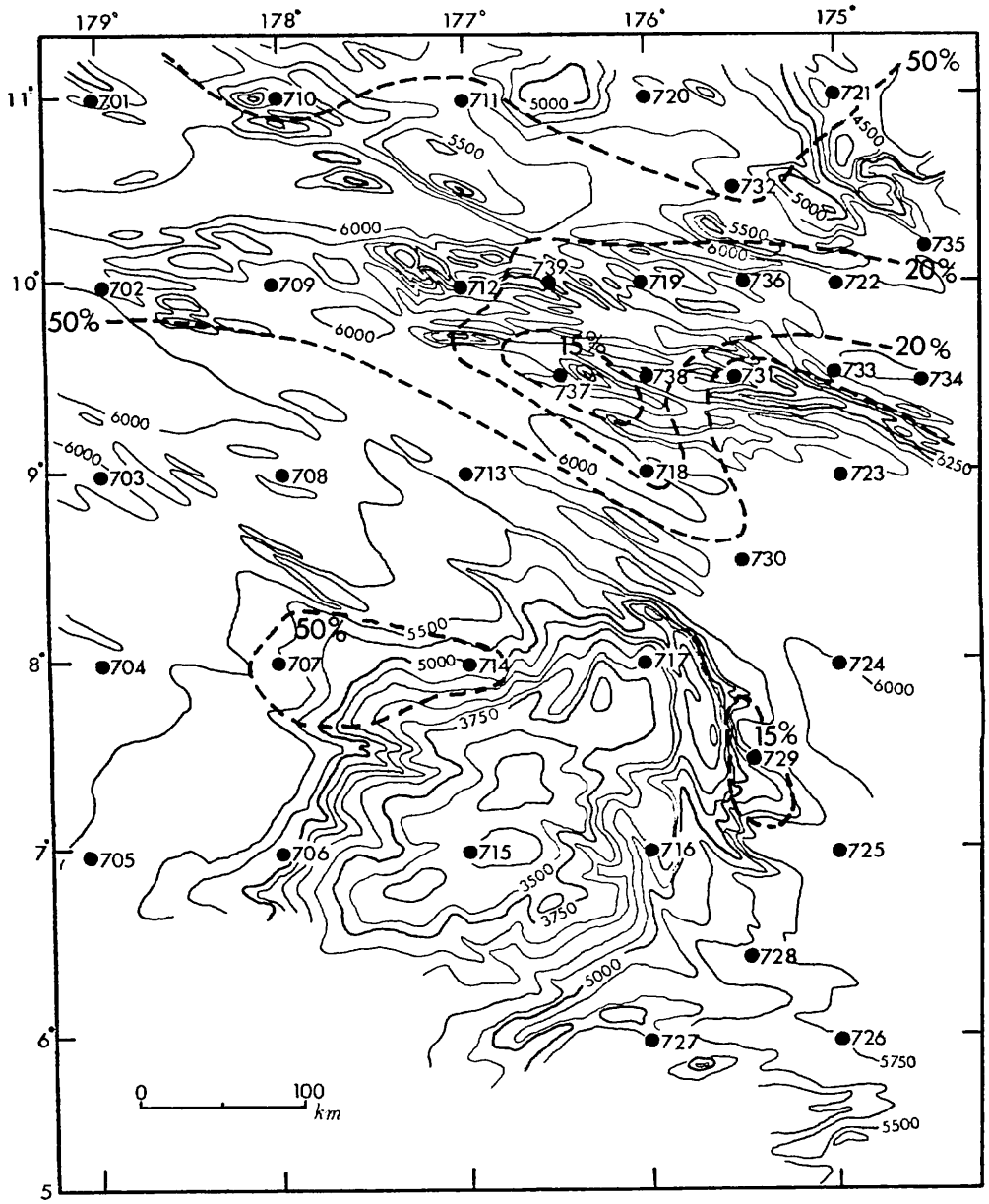

Fig. VIII-8 Grain size distribution of less than 2 cm manganese nodules.

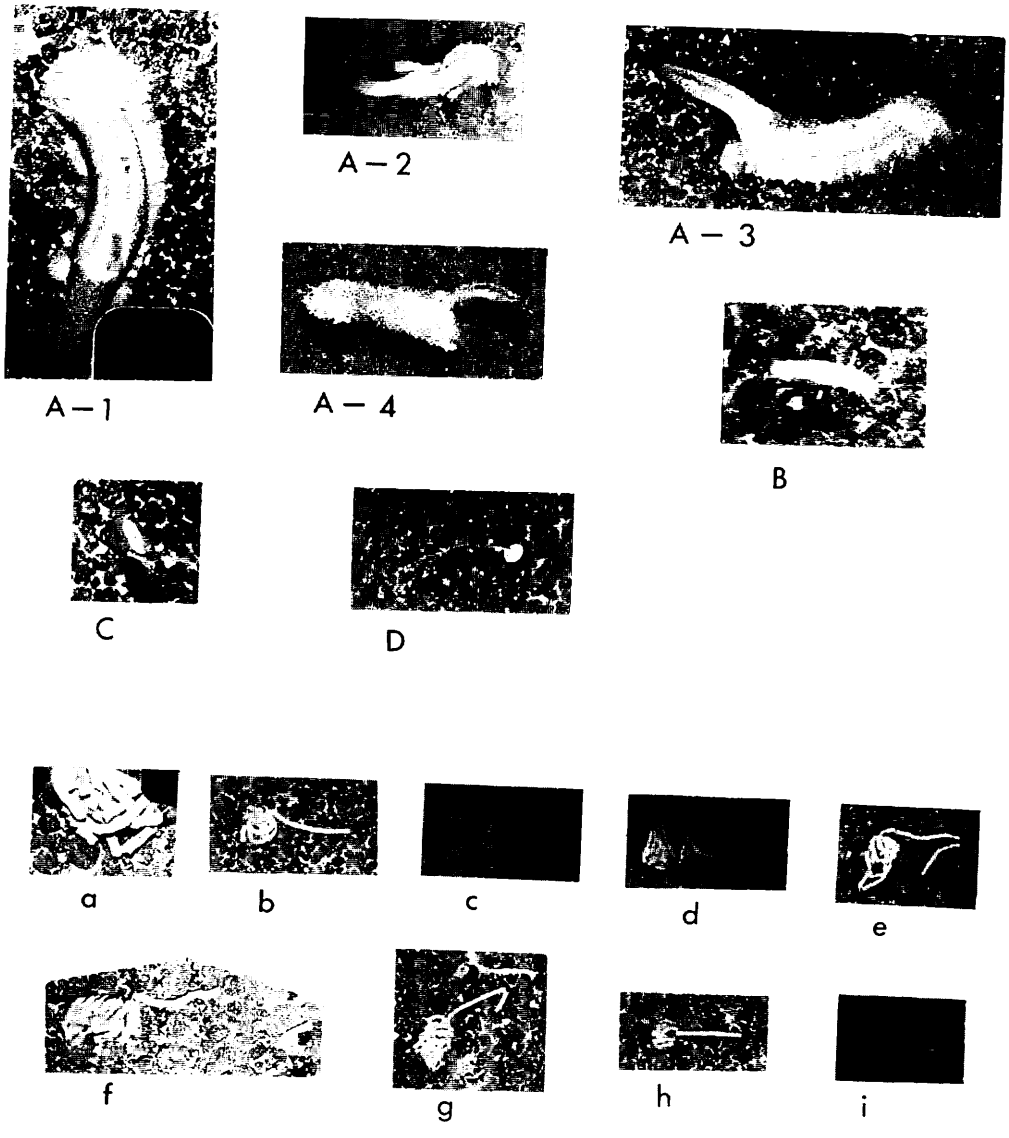

ST. 735 C-11 5,484m - 5,556m

A - D: Benthonic organisms

a - i: Coprolites

Fig. VIII–9 Benthonic organisms and coprolites at St. 735. Individual manganese nodules serve as the relative scale in each figures.

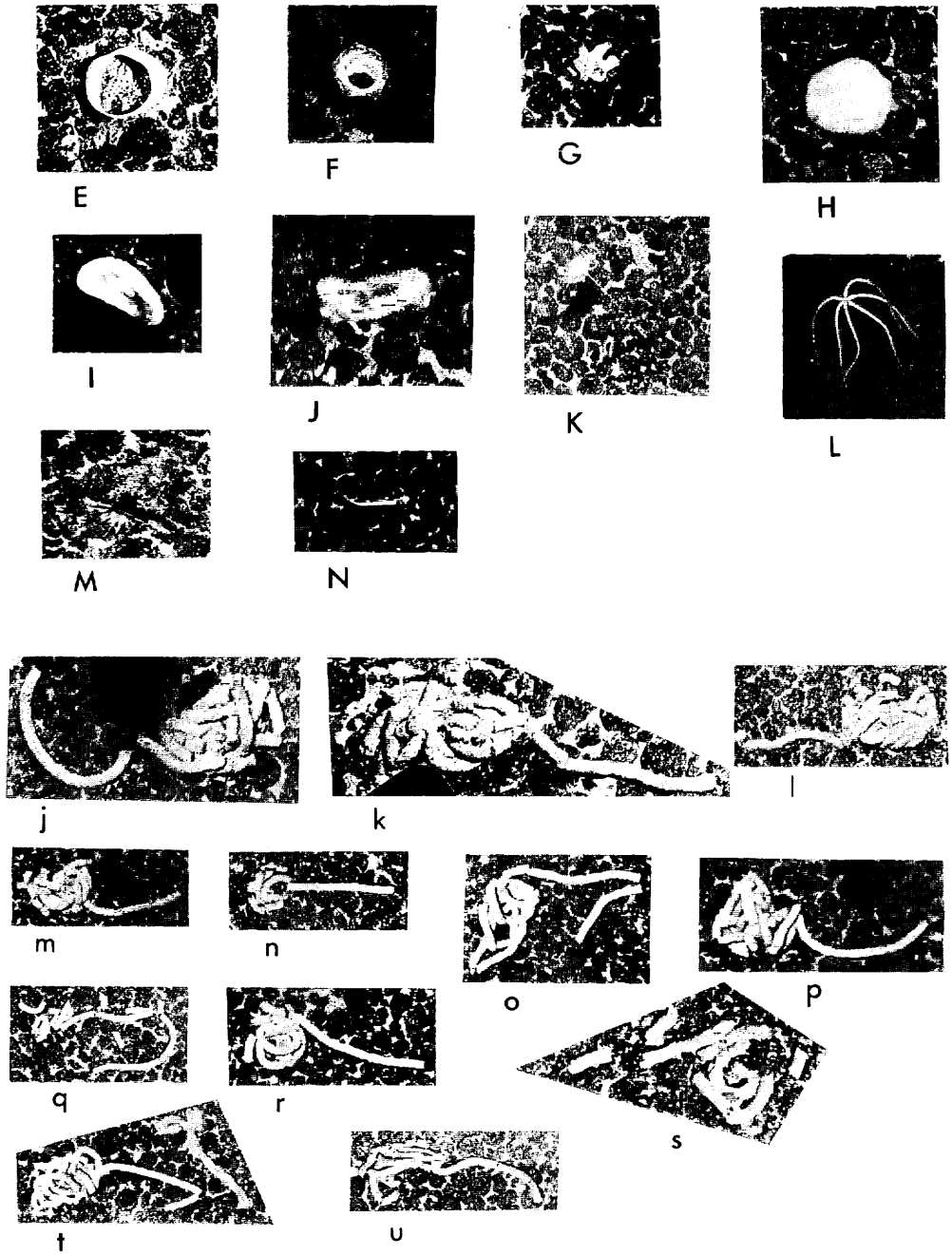

ST. 737 C-12 5,743m

E - N: Benthonic organisms

j - v: Coprolites

Fig. VIII-10 Benthonic organisms and coprolites at St. 737.

In summarizing the distribution of grain size of manganese nodules in relation to the cover ratio, though this may represent only the general and regional tendency because of scarcely spaced sampling stations, and of the cases of existence of abrupt changes in cover ratio within the same station area, it can be mentioned that the higher cover ratio lies around the zonal area between 9°30′–10°30′N and 174°00–177°W, and the relatively larger size nodules such as 8–6 cm and 6–4 cm are found in the central parts of the higher cover ratio area, while smaller size nodules less than 2 cm become abundant towards the marginal parts of the same area. This indicates that the formation of manganese nodules was not uniform throughout the surveyed deep sea bottom areas, but the favorable condition for the concentration of the metal elements was variable horizontally as a whole due to any geological factors.

Benthonic activities

Figs. VIII–9 and VIII–10 show the pictures of benthonic organisms and their traces of activities, taken by the deep sea 35 mm camera at St. 735 (C–11) and St. 737 (C–12) respectively.

The pictures from St. 735 (Fig. VIII–9) show four types of organisms (A, B, C, and D). A–1–4 are similar type of holothurian (sea cucumber) with the size of 40–50 cm length inferred from the nodule size on background. The type of C was also photographed in the GH76–1 cruise (KINOSHITA, 1977).

At St. 737 (C–12), ten types of organisms (E–N in Fig. VIII–10) were found. Among them, E, F, G, H are sponge like organisms, and J looks like a holothurian with evident luminescence.

Pictures of a–i in Fig. VIII–9 and j–u in Fig. VIII–10 are of coprolites. These show a tendency that a rope like coprolite makes both a mount of coil at one end and a projected strech at the other end. Judging from the nodule size on background the length of the coprolits as a whole including the coil mass and the strech part is 50–60 cm, and the width or diameter of the rope of coprolites is 1 cm in most cases.

This kind of coprolites is commonly found in the areas of abundant manganese nodule distribution, with even three or four masses of coprolites within one frame of photograph in some cases. Other types of coprolites are seldom recognized. The similar coprolites were also found at St. 408A–1 in the GH76–1 cruise (KINOSHITA, 1977). Evidences of the activities of benthonic organisms in the deep sea bottom seem to suggest that they may affect significantly on the growth or formation of manganese nodules because the time represented by the activities of benthonic organisms is so enomous as compared with the rate of sedimentation or of formation of manganese nodules.

Reference

KINOSHITA, Y. (1977) Manganese nodules and benthonic activities by deep sea photography. *In* A. MIZUNO and T. MORITANI (*eds.*), *Geol. Surv. Japan Cruise Rept.*, no. 8, p. 78–93.